Journal of Power Sources 214 (2012) 119–123

Contents lists available at SciVerse ScienceDirect

Journal of Power Sources

journal homepage: www.elsevier.com/locate/jpowsour

Short communication

Si–O–C materials prepared with a sol–gel method for negative electrode of lithium battery

Xiang Liu [a,*], Kai Xie [a], Chun-man Zheng [a], Jun Wang [b], Zhaoqing Jing [a]

[a] Department of Materials Engineering and Applied Chemistry, National University of Defense Technology, 410073 Changsha, PR China
[b] Key Laboratory of New Ceramic Fibers and Composites, National University of Defense Technology, 410073 Changsha, PR China

HIGHLIGHTS

► A sol–gel method is used to prepare Si–O–C anode materials.
► The formed materials exhibit a high capacity and good cyclic performance.
► The high capacity comes from lithium storage in SiO_4 units.

ARTICLE INFO

Article history:
Received 17 January 2012
Received in revised form
6 March 2012
Accepted 26 April 2012
Available online 4 May 2012

Keywords:
Lithium anodes
Polymer-derived ceramics
Silicon oxycarbide
Sol–gel method

ABSTRACT

A sol–gel method is employed to prepare high capacity Si–O–C materials. A blend of polysiloxane and divinylbenzene is uniformly spread in the ethanol solution of triethoxysilane and diethoxymethylsilane, which is then hydrolyzed, crosslinked and finally pyrolyzed at 1000 °C in a hydrogen atmosphere to obtain the final composite materials. The resultant materials, as indicated by elemental analysis, mainly consist of Si–O–C glass phase, in which the dominant silicon species is identified to SiO_4 units by ^{29}Si magic angle spinning nuclear magnetic resonance and Si (2p) X-ray photoelectron spectroscopy. The Si–O–C materials exhibit a stable reversible capacity of ca. 900 mAh g^{-1}, originating from lithium storage in SiO_4 units, with a coulombic efficiency of 98.5%.

1. Introduction

Lithium ion batteries are promising power sources to meet growing energy needs. However, the conventional anode material, graphite, has already attained its theoretical capacity. Among several alternatives, polymer-derived silicon oxycarbide (Si–O–C) materials have been extensively studied as potential anode materials in lithium ion batteries. They are usually prepared through a polymer-to-ceramic transformation, the structure of polymer precursor is therefore the key to the structure of pyrolyzed ceramic material. The early researchers focused on pyrolyzing polymer precursors with different structures to form Si–O–C anodes. Phenyl-substituted polysilanes [1] or polysiloxanes [2] were often used as the precursors. Some extra carbon sources were also brought in, e.g. pitch [3], polystyrene [4], and divinylbenzene (DVB) [5], in order to change the elemental composition. Recently, several new processing methods are introduced to prepare high capacity Si–O–C anodes, such as coating the Si–O–C compounds on exfoliated graphite [6]and depositing thin films of polymer-derived silicon oxycarbide on copper [7]. The achieved samples showed large and steady insertion/extraction capacities for lithium ions.

Si–O–C ceramic materials are often described as SiC_xO_y or SiCO. They usually include Si–O–C glass (SiC_xO_{4-x}, where $0 \leq x \leq 4$) and free carbon phase. The free carbon is electrochemically active with lithium and capable of improving the conductivity of the system, but it should not be the major component due to its limited capacity. The Si–O–C phase is believed to be the major electrochemically active site for lithium storage. Our previous work [5] has approved the oxygen-containing silicon species (such as SiO_4 and SiO_3C) in Si–O–C glass phase can reversibly react with lithium. Therefore Si–O–C materials with large content of reversible oxygen-containing silicon species (such as SiO_4 and SiO_3C) but little free carbon are expected to deliver a large reversible capacity. A sol–gel method was employed to prepare the target material in the present paper. A blend of polysiloxane and DVB was uniformly spread in the ethanol solution of triethoxysilane (T^H) and

* Corresponding author. Tel.: +86 731 8457 3149; fax: +86 731 8457 3150.
E-mail address: hu_nan_xiang@yahoo.com.cn (X. Liu).

0378-7753/$ – see front matter © 2012 Elsevier B.V. All rights reserved.
doi:10.1016/j.jpowsour.2012.04.082

diethoxymethylsilane (D^H). They were first hydrolyzed in an ice bath, then crosslinked at higher temperatures and finally pyrolyzed at 1000 °C in a hydrogen atmosphere to obtain the final composite materials. The gel of T^H and D^H was able to form silicon-rich Si–O–C materials with large content of SiO_4 and SiO_3C on pyrolysis [8], which can therefore provide plenty of reversible silicon species for our resulting materials. The structures of the formed material were characterized in depth by scanning electron microscopy (SEM), transmission electron microscopy (TEM), Raman spectra, ^{29}Si magic angle spinning nuclear magnetic resonance (^{29}Si MAS NMR), X-ray photoelectron spectroscopy (XPS). The prepared Si–O–C materials show large lithiation/delithiation capacities.

2. Experimental

2.1. Synthesis of anode powder

Gels were obtained by hydrolysis and condensation reactions of a 9:1 M mixture of T^H, $HSi(OEt)_3$, and D^H, $HCH_3Si(OEt)_2$. This particular composition was chosen because it leaded to the formation of silicon-rich silicon oxycarbide glass on pyrolysis [8]. Weighted amounts of the two alkoxides (TCI, China) were mixed in ethanol ($E_tOH/Si = 2$). The mixture was then mixed with the blend of DVB and polysiloxane (1:1 in weight). The polysiloxane was reported in our previous paper [9]. Its structures is $Si(CH_3)_3(Si(OH)(CH_3)O)_i(Si(C_6H_5)(CH_3)O)_j(Si(CH_3)(H)O)_k(Si(CH_3)Si(C_3H_7)_2O)_lSi(CH_3)_3$ (where, i, j, k, $l > 1$). The blend was then hydrolyzed with distilled water ($H_2O/OR = 1$; $pH = 4$). The solution was stirred for 3 h in an ice bath, and then for another half an hour at 70 °C to complete gelation and crosslink. White, monolithic gels were then obtained. The crosslinked samples were then further crosslinked at 300 °C for 6 h in an inert atmosphere. Black glasses were produced from the crosslinked samples by a pyrolysis process at 1000 °C in a flowing hydrogen atmosphere (200 mL min^{-1}). Samples were placed in a furnace equipped with a silica tube and heated 5 °C min^{-1} with a holding time of 1 h at the maximum temperature.

Silicon content of the pyrolysis product was determined by a fusion technique which consisted of converting the solid to a soluble form and analyzing the solute for total silicon with a Varian 715-ES analysis. Carbon content was measured in FlashEA1112 elemental analyzer (Thermo Electron SPA). The oxygen fraction was calculated as the difference to 100% of the sum of the wt%-values of silicon and carbon, assuming a small amount of hydrogen in the analyzed samples and no other elements present. The amount of free carbon (i.e., that not bound to silicon, or oxygen) in the product was calculated by subtracting the theoretical amount of carbon bound to silicon from the total carbon. The carbon and silicon content of the pyrolyzing samples at 1000 °C is 22.7 and 37.4 wt%, respectively. The calculated free carbon content is 21.6 wt %. So the average composition from elemental analysis is $SiO_{1.87}C_{1.43}$.

A S4800 instrument was used to perform SEM investigation on the ball-milled powders of the materials and a JEOL JEM-3010 instrument was used to perform TEM investigations on fine powders dispersed on a copper grid. Raman spectra were recorded on an Advantage 532 (DeltaNu) equipped with a microscope and a Charge-coupled Device (CCD) detector. Excitation was by means of a green laser of 532 nm.

An XPS spectrum was used to determine the chemical bonding state and the composition of the Si–O–C material using VG Multilab2000 (Thermo Fisher Scientific). The X-ray source was a monochromatized Al Ka line with a power of 240 W (12 kV and 20 mA). An Ar^+ beam sputtering was applied to etch away the surface of the materials to eliminate any possible surface contamination. The analysis of the samples yielded values for Si (2p), O (1s) and C (1s).

^{29}Si MAS NMR spectrum was collected on an AVANCE III spectrometer (Bruker) at 79.49 MHz. A pulse width of4.50 μt ($\theta = 45°$) and a recycle delay of 30 s were used for single pulse without a cross polarization technique. Samples were finely ground and packed into ZrO_2 rotors (7-mm diam) and spun (6 kHz). All chemical shifts (δ) were referenced to tetramethylsilane (TMS; $\delta = 0$).

2.2. Half-cell preparation

Si–O–C composite anodes of about 25 μm thick were prepared by coating slurries of the pyrolyzed powders (80% by weight), Acetylene Black (10% by weight), and polyvinylidene fluoride (PVDF) dissolved in *N*-methyl pyrrolidinone on copper foil substrates. After coating, the electrodes were dried overnight at 110 °C in air and then pressed between flat plates at about 15,000 kPa pressure. Coin-type test cells (four for each sample) were constructed from the electrodes. The electrolyte used was 1 M $LiPF_6$, dissolved in a 50/50 v/v% mixture of ethylene carbonate (EC) and diethyl carbonate (DEC). A microporous film (Celgard 2400) wetted with the electrolyte was sandwiched between the active electrode and a Li metal foil anode. Cells were assembled in an argon-filled glove box. Electrochemical testing of the cells was performed using constant current cyclers whose currents are stable to ±1%. The cells were placed in thermostats at 30 °C. Cells were discharged first with a constant current of 50 mA g^{-1}. When the cell discharge potential reached 0.001 V, the current direction was

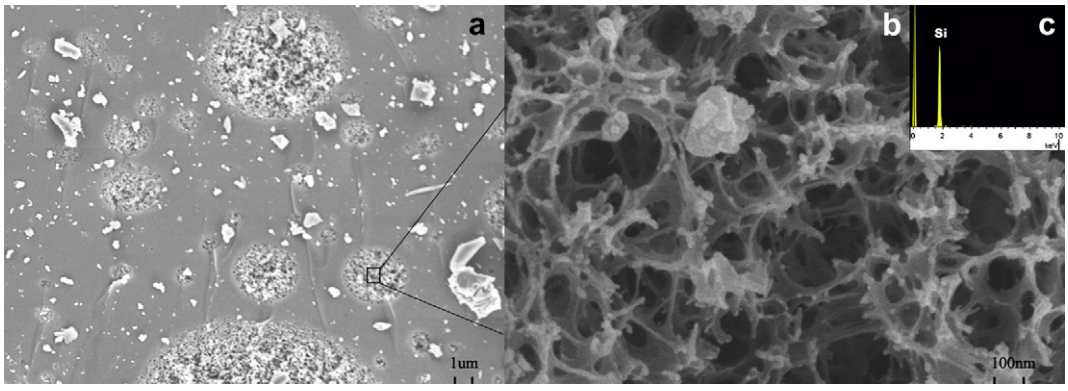

Fig. 1. (a) SEM micrograph, (b) the enlarged graph of the selected area, and (c) the EDS spectra of the Si–O–C materials prepared by sol–gel method.

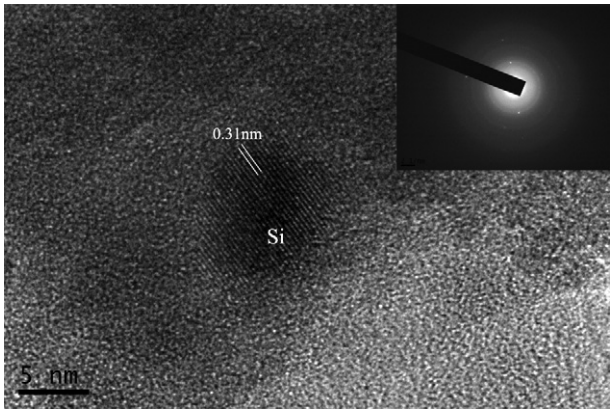

Fig. 2. High-resolution TEM micrograph of the Si–O–C materials prepared by a sol–gel method at 1000 °C.

reversed and the cells were in the charge mode. Upon current reversal, Li was removed from the active anode. Charging of the cells was considered complete when the cell potential reached 3.0 V. The reversible capacity is defined as the average of the first charge and second discharge capacity.

3. Results and discussion

Fig. 1 shows the SEM micrograph of the Si–O–C material prepared with a sol–gel method in a hydrogen atmosphere. Fig. 1 (a) shows the typical surface of the particles of the materials. Most of the particles have solid surface, with some irregular minor particles on it. Some round porous cavities are also observed on the surface, though they only account for a minor fraction of the materials. From the enlarged graph in Fig. 1 (b), the porous regions are full of nanothreads, which are almost composed of elemental silicon confirmed by Electron dispersive Spectrometer (EDS) analysis in Fig. 1 (c).

Fig. 2 shows the TEM image of the formed Si–O–C material. Most of the material is amorphous Si–O–C phase, confirmed by a diffuse ring at about 4 Å [10]. Some crystalline planes with d-spacing of 0.31 nm corresponded to (111) planes of elemental silicon (PDF#27–1402) embedded in the amorphous matrix. The close contact between the silicon and Si–O–C matrix is good for the improvement of capacity retaining of silicon.

Fig. 3 shows the Raman spectra of the Si–O–C materials prepared with a sol–gel method. Two modes associated with free carbon are clearly observed, which confirms the formation of free carbon nanodomains. The first mode at 1611 cm^{-1}, often referred as the G mode, is assigned to 'in plane' displacement of the carbons strongly coupled in the hexagonal sheets. The other mode at

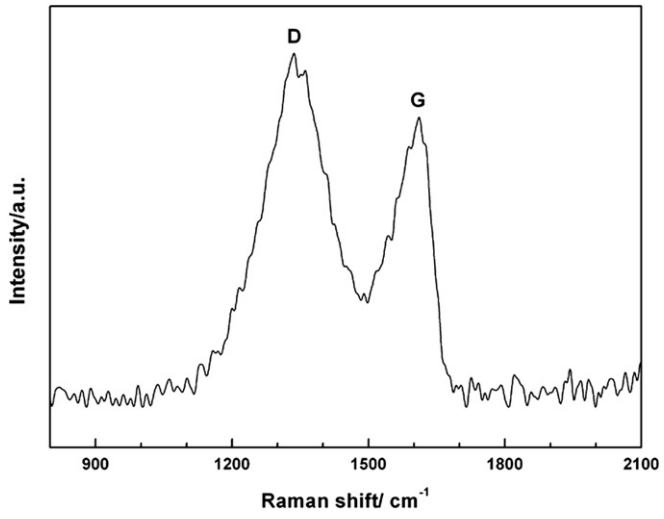

Fig. 3. Raman spectra of the Si–O–C materials prepared by a sol–gel method at 1000 °C.

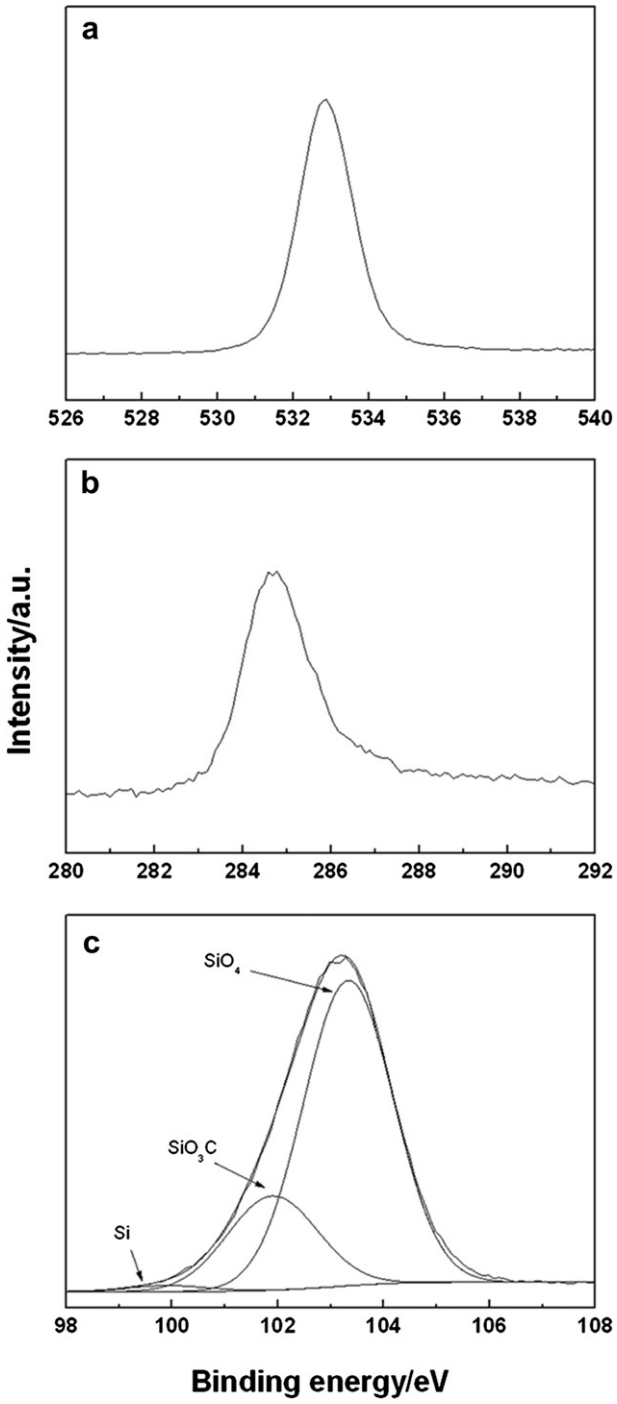

Fig. 4. XPS spectra of the Si–O–C materials prepared by a sol–gel method at 1000 °C: (a) O (1s), (b) C (1s) and (c) Si (2p).

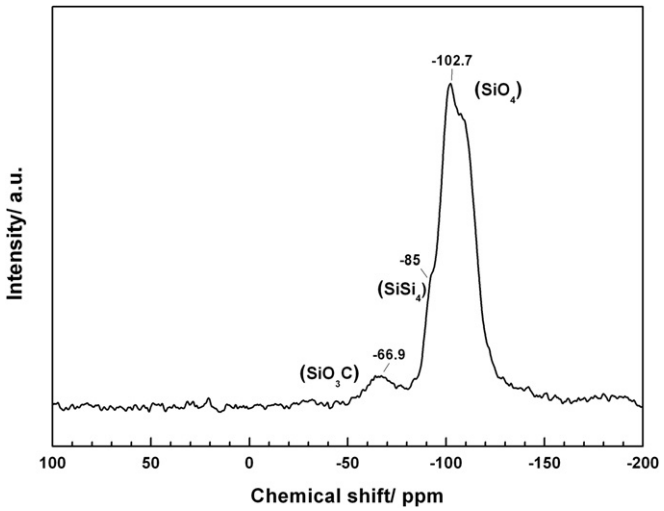

Fig. 5. ^{29}Si MAS NMR spectra of the Si–O–C materials prepared by a sol–gel method at 1000 °C.

1338 cm^{-1} is characteristic of C–C single bonds between sp^3-hybridized carbon atoms. The formation of free carbon is related with the breaking of C–H bonds. In comparison with the carbon bonded to silicon, the C–H bonds in the precursor are easy to break on pyrolysis. Thus hydrogen is released, leaving behind excess carbon (free carbon) in the ceramic. The free carbon can improve the conductivity of the material, and also act as a buffer to alleviate the volume change during lithium insertion/distraction. In addition, no peaks at about 520 cm^{-1} assigned to elemental silicon in the Raman spectra is observed due to its minor content, as will be seen in Si(2p) XPS and ^{29}Si MAS NMR spectra later.

An XPS spectrum is usually used to determine the chemical bonding state and the composition of the Si–O–C material. Fig. 4 shows the XPS spectra of the Si–O–C materials prepared with a sol–gel method. An Ar^+ beam sputtering was applied to etch away the surface of the materials to eliminate any possible surface contamination. Fig. 4 (a) shows the O (1s) XPS spectra of the material. The symmetry peak centered at 532.9 eV can be assigned to –Si–O–Si– units [11], confirming the oxygen atom in the materials is always bonded to silicon atoms. From Fig. 4 (b), the C (1s) peak is centered at 284.6 eV, which can be assigned to C–C bonds in the free carbon matrix [12]. It is consistent with the previous Raman analysis. No peaks at 282.8 eV were observed, suggesting the absence of CSi_4 units.

Fig. 4 (c) shows the Si (2p) spectra of the formed Si–O–C composite material. The broad peak can be fitted into three peaks: the largest peak is centered at 103.1 ev, which can be assigned to SiO_4 units [12]. Another peak at 102.1 eV is corresponding to SiO_3C units [12]. And the other peak at 99.5 eV is surely assigned to elemental silicon. Fig. 5 shows the ^{29}Si MAS NMR spectra of the same materials. Three peaks at −102.7, −85, and −66.9 ppm are corresponding to SiO_4, $SiSi_4$, and SiO_3C units [8], respectively, which are consistent with the Si (2p) XPS analysis. No other silicon species are observed. According to Si (2p) XPS and ^{29}Si MAS NMR analysis, SiO_4 units are the major silicon species and the electrochemically active SiO_3C units also contribute reasonable part of the weight. The elemental silicon is least in comparison with the above silicon species.

Fig. 6 (a) shows the first two discharge/charge curves of the anode using the formed Si–O–C material as the active material. These data were obtained at a current density of 50 mA g^{-1} between the voltage limits of 0.001 and 3 V. The discharge represents a direction where lithium species are inserted into the composite anode, and the charge represents the opposite direction. It can be seen that the anode offers a first discharge capacity of 1726.8 mAh g^{-1}, of which 1190.7 mAh g^{-1} is reversible, giving a first coulombic efficiency of 69%. After cycled 20 times, as is seen in Fig. 6 (b), it still retains a stable capacity of ca.900 mAh g^{-1} at 50 mA g^{-1}, with a coulombic efficiency of 98.5%. The reversible capacity is believed to origin from the lithium storage in electrochemically active silicon units and free carbon. Considering free carbon only accounted for 21.6 wt% of the total weight and amorphous carbon was known to deliver a capacity of ca. 440 mAh g^{-1} [13], the reversible capacity of lithium insertion in the Si–O–C sample mostly comes from lithium reaction with the silicon species. Furthermore, of all the silicon species, the SiO_4 units account for the major part of the total weight, confirmed by ^{29}Si MAS NMR of the material. So it can be reasonably concluded the lithium storage in SiO_4 units contribute to most of the capacity, and its specific capacity is at least 900 mAh g^{-1}. However, thin film of crystalline SiO_2 was reported to only offer a reversible capacity in the range of 416–510 mAh g^{-1} [14]. The much larger capacity of SiO_4 units in our samples may be related with nanostructure of the Si–O–C materials. From the nanodomain model [15], SiO_4 units are surrounded by the intermediate mixed silicon oxycarbide species, SiC_xO_{4-x}, ($0 \leq x < 4$), which are then enwrapped by free carbon wall. Both the mixed bond tetrahedral silicon species and free carbon wall can alleviate the volume change of lithium insertion in SiO_4 units, which is good for the improvement of Lithium insertion/distraction ability of SiO_4 units. Besides, the intermediate mixed silicon species, SiO_3C units, are also known to be electrochemically

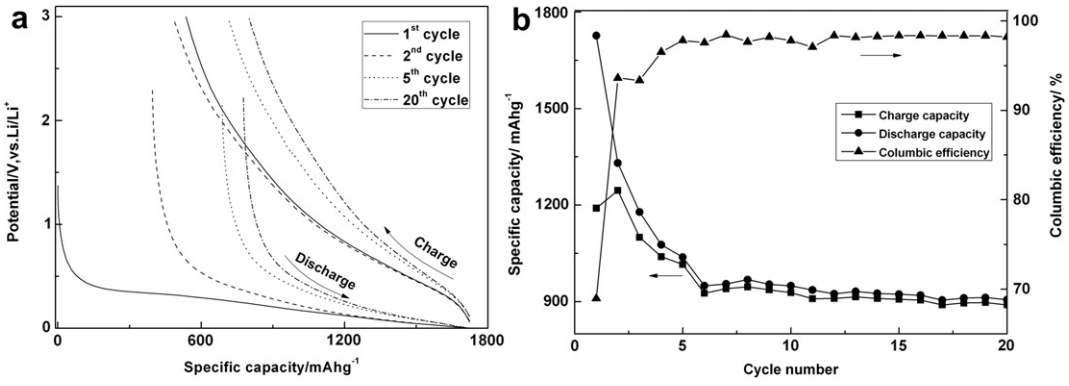

Fig. 6. (a) First two discharge/charge curves and (b) cyclic performance of the prepared Si–O–C anode by sol–gel method at 1000 °C. The current is 50 mA g^{-1}.

reversible with lithium and can contribute to the reversible capacity [5]. In addition, the crystalline silicon, which has a theoretical specific capacity of 4200 mAh g^{-1} [16], could also contribute to some of the capacity, though its content was minor. From SEM and TEM micrograph, the crystalline silicon is enwrapped by amorphous Si–O–C matrix, which could act as a buffer to alleviate volume change of lithium insertion in silicon and then maintain high capacity of the materials.

4. Conclusions

We have prepared high capacity Si–O–C materials utilizing a sol–gel method. The general preparation routine was as follows: A blend of polysiloxane and DVB (1:1 in weight) was uniformly spread in the ethanol solution of triethoxysilane and diethoxymethylsilane, which was then hydrolyzed in an ice bath. After the hydrolyzed sample was crosslinked at higher temperatures and then pyrolyzed at 1000 °C in a hydrogen atmosphere, the final Si–O–C material was achieved. The resultant materials, as indicated by elemental analysis, are mainly composed of Si–O–C glass phase, in which SiO4 units are the major silicon species, confirmed by Si (2p) XPS and ^{29}Si MAS NMR spectra. A small amount of elemental silicon also exists in the samples. The Si–O–C material exhibits a stable reversible capacity of ca.900 mAh g^{-1} at 50 mA g^{-1}, with a coulombic efficiency of 98.5%. Most of the capacity reasonably comes from lithium storage in SiO_4 units, though the mechanism is still unknown.

References

[1] A.M. Wilson, J.N. Reimers, E.W. Fuller, J.R. Dahn, Solid State Ionics 74 (1994) 249–254.
[2] L. Ning, Y. Wu, L. Wang, S. Fang, R. Holze, J. Solid State Electrochem. 9 (2005) 520–523.
[3] A.M. Wilson, W. Xing, G. Zank, B. Yates, J.R. Dahn, Solid State Ionics 100 (1997) 259–266.
[4] H. Fukui, H. Ohsuka, T. Hino, K. Kanamura, ACS Appl. Mater. Interfaces 2 (2010) 998–1008.
[5] X. Liu, M.-C. Zheng, K. Xie, J. Power Sources 196 (2011) 10667–10672.
[6] H. Konno, T. Morishita, C. Wan, T. Kasashima, H. Habazaki, M. Inagaki, Carbon 45 (2007) 477–483.
[7] J. Shen, R. Raj, J. Power Sources 196 (2011) 5945–5950.
[8] G.D. Soraru, G. D'Andrea, R. Campostrini, F. Babonneau, G. Mariotto, J. Am. Ceram. Soc. 78 (1995) 379–387.
[9] X. Liu, M.-C. Zheng, K. Xie, J. Liu, Electrochim. Acta 59 (2012) 304–309.
[10] H. Bréquel, J. Parmentier, S. Walter, R. Badheka, G. Trimmel, S. Masse, Chem. Mater. 16 (2004) 2585–2598.
[11] J.F. Moulder, W.F. Stickle, P.E. Sobol, K.D. Bomben, Handbook of X-Ray Photoelectron Spectroscopy: a Reference Book of Standard Spectra for Identification and Interpretation of Xps Data, second ed. Physical Electronics Division, Eden Prairie, 1992.
[12] G.D. Sorarh, G.D. Andrea, A. Glisenti, Mater. Lett. 27 (1996) 1–5.
[13] S. Wang, Y. Matsumura, T. Maeda, Synth. Met. 71 (1995) 1759–1760.
[14] Q. Sun, B. Zhang, Z.-W. Fu, Appl. Surf. Sci. 254 (2008) 3774–3779.
[15] A. Saha, R. Rajw, D.L. Williamson, J. Am. Ceram. Soc. 89 (2006) 2188–2195.
[16] B.A. Boukamp, G.C. Lesh, R.A. Huggins, J. Electrochem. Soc. 128 (1981) 725–729.